High Gain, Wideband Aperture Coupled Microstrip Antenna Design Based on Gain-Bandwidth Product Analysis

M. M. Bilgic [1] and K. Yegin [2]

[1] Unitest Inc., Kadıköy, Istanbul 34722, Turkey
mustafamuratbilgic@gmail.com

[2] Department of Electrical and Electronics Engineering
Ege University, Izmir 35040, Turkey
yegink@gmail.com

Abstract ─ Aperture coupled antennas are studied in terms of Gain-Bandwidth Product (GBWP). To understand whether resonant or non-resonant slot coupled antenna has better performance, several antenna designs with different slot shapes are optimized and compared to each other. Even for a pin-feed microstrip antenna, we show that there exists a substrate height and aspect ratio for optimal GBWP. Based on this analysis, a stacked aperture coupled antenna is designed and optimized for high gain and wideband for Ku band downlink (10.8-12.75 GHz) applications. The designed antenna exhibits 9.5 dBi broadside gain with 80° half power beam width and almost 30% bandwidth. Ku-band gain ripple is less than 0.5 dB. The antenna is built and measured. Several figure-of-merits based on GBWP have been defined to compare its performance with earlier works. Proposed antenna can be used in demanding high gain, wideband, beam scanning array applications.

Index Terms ─ Aperture coupling, gain-bandwidth product, Ku band, microstrip antenna, satellite TV.

I. INTRODUCTION

High gain and wideband planar antennas are essential to satisfy system requirements in many wireless systems. Once target bandwidth is achieved in the design, antenna gain becomes the next goal, because gain directly impacts Signal-to-Noise Ratio (SNR) of the system. Often, minimum gain in the target bandwidth is specified to fulfill SNR requirement. However, gain and bandwidth are usually complementary metrics such that improving one degrades the other. Thus, one must optimize the design for Gain-Bandwidth Product (GBWP) rather than bandwidth only. An upper bound on gain-bandwidth product can be placed for electrically small antennas [1], but this is rather difficult for multiple resonant or wideband antennas.

One of the most common planar antenna configurations is the Slot Coupled Microstrip Antenna (SCMSA) configuration [2]. Slot coupling is also suitable for high frequency applications where structural dimensions are in millimeter or sub millimeter range. Most of these applications require high directive gain; thus, utilize phased arrays where high gain and wideband antenna elements are required. To increase the bandwidth of SCMSA, parasitic elements in the form of stacked patches or coplanar parasitic elements were proposed [3-4]. Unlike coplanar parasitic elements, stacked patches do not increase the aperture area of the antenna; hence, does not require increased inter-element spacing that may cause grating lobes. Either a non-resonant slot is coupled to stacked resonant patches or a resonant slot radiates with resonant stacked elements. Stacked patches coupled with a resonant slot exhibited Fractional Bandwidth (FBW) in excess of 50%, with gain in excess of 5 dBi [5-6]. For non-resonant slot coupling, various slot shapes ranging from rectangular slots to dog-bone shape slots have been proposed [2-9]. Hourglass shape non-resonant slot was identified as the best configuration in terms of fractional bandwidth [3]. However, none of these studies considered GBWP, and which

Submitted On: June 24, 2013
Accepted On: July 23, 2014

configuration produces best gain-bandwidth performance is yet unknown. Also, it is still unclear whether resonant slot or non-resonant slot has better performance.

In any antenna design, bandwidth, gain, and HPBW are the most essential design characteristics along with other features, such as cross-polarization ratio, front-to-back ratio, in-band gain ripple, electrical height, and physical dimensions. Although, it is difficult to define a common Figure-of-Merit (FOM) to combine all these metrics into one, we defined several FOM's based on GBWP. We compare performances of various non-resonant and resonant slot coupled stacked patches to identify the best configuration in terms of these FOM's. We are particularly interested in Ku band applications for mobile satellite TV reception. We derive a wideband equivalent circuit representation of SCMSA to study the impact of design parameters on bandwidth. Based on this study, we propose a high gain, wideband antenna structure operating at Ku band with highest FOM compared to earlier works.

Specific contributions of this study are:

i) GBWP analysis of microstrip and aperture coupled antennas.
ii) Comparison of resonant versus non-resonant slot coupled antennas.
iii) Determination of slot shape that provides best performance.
iv) Design of a non-resonant slot coupled antenna with high FOM.

We derive GBWP for single mode rectangular patch antenna in the next section. Aperture coupled antennas and their equivalent circuit representations are presented in Section III. Ku Band antenna element design is detailed in Section IV. FOM definitions and comparison table are given in Section V. Conclusions are presented in Section VI.

II. GAIN-BANDWIDTH PRODUCT OF RECTANGULAR PATCH ANTENNA

The bandwidth for a rectangular patch antenna with length L, width W and substrate height h is given as:

$$BW = \frac{VSWR-1}{Q\sqrt{VSWR}}\,, \tag{1}$$

where Q represents the quality factor of the patch. Fractional bandwidth rather than absolute bandwidth is regarded as the bandwidth; thus, BW can also be expressed as:

$$BW = \frac{f_U-f_L}{f_C}\,, \tag{2}$$

where f_U, f_L, and f_C represent upper, lower and center frequency of the impedance match frequency band. For $VSWR$=2, BW becomes:

$$BW = \frac{1}{Q\sqrt{2}}\,. \tag{3}$$

For electrically thin substrates ($h/\lambda \ll 1$), BW can be estimated as [10]:

$$BW = \frac{16}{6\pi\sqrt{2}}\frac{c_1 p}{e_r}\frac{k_0 h}{\varepsilon_r}\frac{W}{L}\,, \tag{4}$$

where e_r is the efficiency, $k_0=2\pi/\lambda_0$ (free space wavenumber), ε_r is the permittivity of the substrate, c_1 and p are functions used in the approximation [10]. For $W/L<2$, p becomes almost 1, and c_1 becomes 0.4 for air-dielectric and nearly 1 for high permittivity substrates. It is clear from (4) that the electrical height of the antenna is directly proportional to the bandwidth. For a given substrate height, the bandwidth is relatively wider at higher frequencies.

The gain of the patch antenna is approximated as [11]:

$$G = \frac{4(k_0 W)^2}{\pi\eta_0} e_r R_r\,, \tag{5}$$

where R_r represents radiation resistance. R_r given in [10] was not very accurate as stated by its authors, so a more accurate representation given in [12] has been used. R_r is proportional to:

$$R_r \sim \varepsilon_r \frac{1}{(k_0 h)^2 \left(k_0 W/2\right)^2 \left[-1+14/\left(k_0 W/2\right)^2\right]}\,. \tag{6}$$

The gain of the antenna is inversely proportional to $(k_o h)^2$. Hence, neglecting the constants and assuming p equals to 1, GBWP for rectangular patch is proportional to:

$$GBWP \sim \frac{1}{k_0 h}\frac{W}{L}\frac{1}{\left[-1+\frac{14}{\left(k_0 W/2\right)^2}\right]}\,. \tag{7}$$

Therefore, increasing $k_o h$ for bandwidth improvement deteriorates attainable gain and limits GBWP. High aspect ratio (W/L) also improves GBWP if higher order modes are not excited. It is interesting to see that substrate permittivity and antenna efficiency are not the factors of GBWP.

Although, these approximate formulas have been widely accepted, they are only valid for electrically thin substrates. We performed 3D simulations on rectangular patch antenna with pin feed and defined GBWP as:

$$GBWP = \frac{\int_{f_L}^{f_U} G(f)df}{f_U - f_L}\left(\frac{f_U - f_L}{f_C}\right)\frac{\sum_{i=1}^{N} G(f_i)\Delta f}{N\Delta f}\left(\frac{f_U - f_L}{f_C}\right) = G_{AVG}BW, \quad (8)$$

where $f_L=f_1 \le f_i \le f_N=f_U$, i=1,2...N and $G(f)$ represents gain (linear, not decibel) as a function of frequency. Rectangular patch antenna is optimized for best GBWP for different k_oh's and relative substrate permittivity's ε_r. We used Nelder-Mead Simplex algorithm for the optimization. The results are shown in Fig. 1. Unlike approximate formulas, simulations show that GBWP has a maximum at certain k_oh and changes considerably with ε_r. We also run similar analysis for different patch aspect ratios for air-dielectric patch, as shown in Fig. 2. Again, it appears that there exists an optimum electrical height where GBWP is optimal. All simulations were run around Ku-band downlink frequency band (10.8-12.75 GHz).

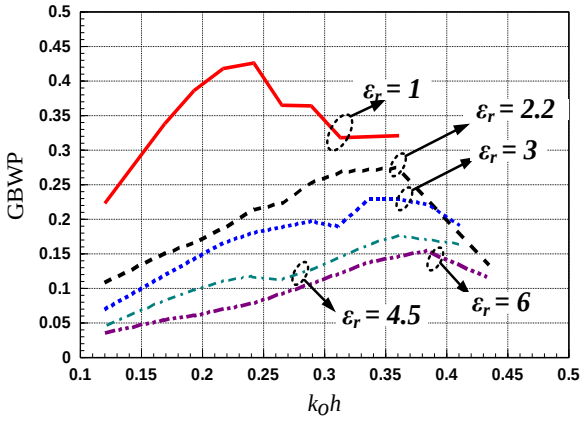

Fig. 1. GBWP for different dielectric materials.

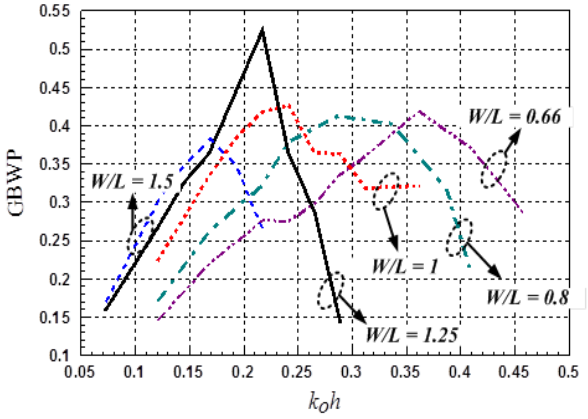

Fig. 2. GBWP for different aspect ratios.

We also compared GBWP performance of pin-feed rectangular patch antenna to that of non-resonant rectangular slot coupled patch antenna and the results are displayed in Fig. 3. We observe that slot-coupled geometry produces much better GBWP performance, as the inductance of the pin feed severely limits BW of the antenna.

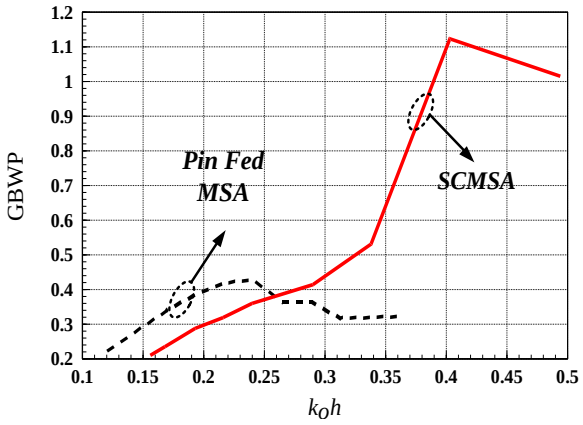

Fig. 3. GBWP for aperture coupled (non-resonant slot) microstrip antenna and pin-feed Microstrip Antenna (MSA), where antenna and feed substrates are air and aspect ratio is 1.

III. APERTURE COUPLED ANTENNAS

A typical aperture coupled antenna configuration with possible aperture shapes is illustrated in Fig. 4. The feed line substrate is Nelco NX9300 (ε_r=3, tanδ=0.0023) with 0.5 mm thickness. Radiating and parasitic patches are placed above the slot plane, suspended in air, at h_1 and h_2, respectively. The feed line is tuned to 50 ohms, and open circuited stub is used to give the desired impedance match. The heights of the suspended patches are 1 mm for the radiating patch and 3 mm for the parasitic patch (measured from the slot plane). As it is evident from the configuration, there are too many structural parameters involved in antenna performance. Equivalent circuit representation of this structure is shown in Fig. 5. Coupling between the patches and patch-to-ground are expressed in terms of jXM_1 and jXM_2 (capacitive coupling). These two impedances are particularly important to achieve wideband corroboration of the circuit model with the results of a 3D electromagnetic solver. The input impedance of the circuit is derived as:

$$Z_{in} = Z_0 \frac{Z'_{in} + jZ_0 tan(\beta_{eff} L_{feed})}{Z_0 + jZ'_{in} tan(\beta_{eff} L_{feed})}, \quad (9)$$

where β_{eff} is calculated for effective dielectric constant of material and Z'_{in} is given by:

$$Z'_{in} = Z''_{in} + jZ_0 tan(\beta_{eff} L_{stub}), \quad (10)$$

and Z''_{in} is:

$$\zeta_1 = Z_{ap} Z_{rp} (n_1^2 Z_{M1} + Z_{pp}), \quad (11)$$

$$\zeta_2 = (n_1 n_2)^2 Z_{ap} Z_{M2} (Z_{rp} + Z_{M1}), \quad (12)$$

$$\zeta_3 = n_2^2 Z_{pp} Z_{ap} Z_{M2}, \quad (13)$$

$$\zeta_4 = n_3^2 Z_{rp} (n_1^2 Z_{M1} + Z_{pp}), \quad (14)$$

$$\zeta_5 = (n_1 n_2 n_3)^2 (Z_{rp} + Z_{M1})(Z_{M2} + Z_{ap}), \quad (15)$$

$$\zeta_6 = (n_2 n_3)^2 Z_{pp} (Z_{M2} + Z_{ap}), \quad (16)$$

$$Z''_{in} = \frac{\zeta_1 + \zeta_2 + \zeta_3}{\zeta_4 + \zeta_5 + \zeta_6}. \quad (17)$$

Z_{ap}, Z_{rp}, Z_{pp}, Z_{M1}, Z_{M2}, n_1, n_2 and n_3 were calculated using relations in [13-15].

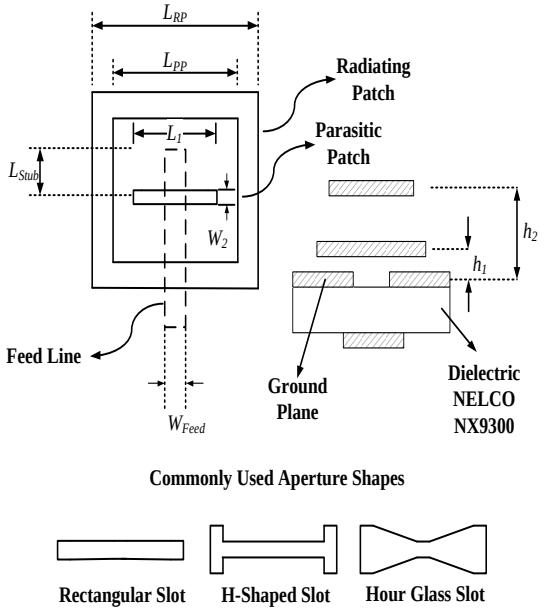

Fig. 4. Aperture coupled antenna and possible aperture shapes.

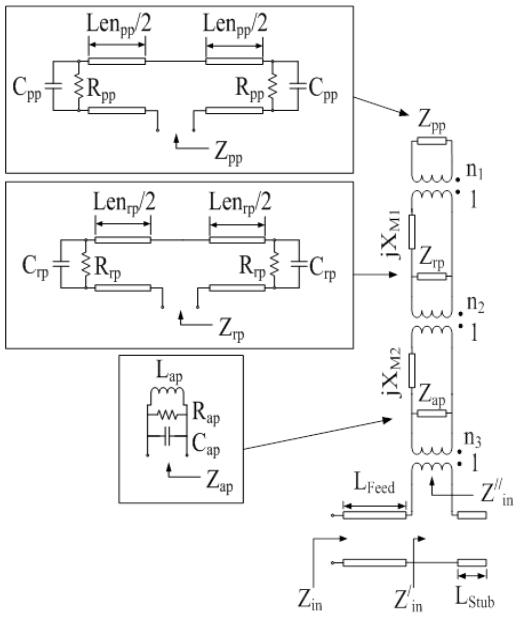

Fig. 5. Equivalent circuit representation of aperture coupled antenna.

Antenna structures are modeled and simulated using FEKO, a commercial electromagnetic field solver based on Method of Moments. For non-resonant slot coupling, rectangular, H-shaped and hourglass slot dimensions are optimized for bandwidth performance. Simplex algorithm within FEKO was used as the optimization tool. Input reflection coefficient for all non-resonant slot coupled antennas and equivalent circuit model for rectangular slot coupled antenna are shown in Fig. 6. We observe that there is a small difference between non-resonant slots for bandwidth (VSWR<2). Equivalent circuit model has fairly close performance to that of rectangular slot. Thus, broadband circuit model of rectangular slot coupled antenna has been verified. Perturbation analysis on structural dimensions reveals that parasitic patch dimensions, slot length and patch heights are more influential on bandwidth; whereas, slot width, resonant radiating patch dimensions are less important.

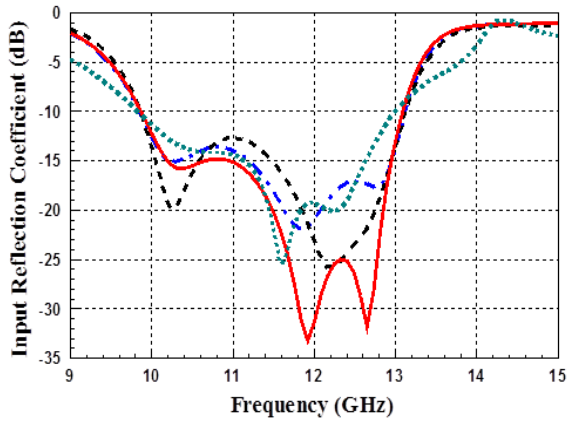

Fig. 6. Input reflection coefficient of aperture coupled antennas and equivalent circuit model (rectangular slot, H-shaped slot, hour-glass shaped slot, equivalent circuit model of rectangular slot).

To compare antenna performances, we defined FOM_1 as GBWP without considering the electrical height and Half-Power Beamwidth (HPBW) of the antenna.

We also studied resonant slot coupled patch antenna, pin-feed Microstrip Antenna (MSA) and resonant slot with two stacked patches (3 resonators), all optimized for performance. The results are shown in Table 1.

Table 1: Comparison of antenna parameters

Antenna	Gain (dBi)	*BW*	k_0h	FOM_1
H-Shaped Slot	7.87-9.06	0.275	0.837	2.088
Hour Glass Slot	7.88-9.07	0.283	0.837	2.150
Rectangular Slot	7.89-9.04	0.275	0.837	2.083
Resonant Slot	3.51-9.19	0.350	0.736	2.142
3 Resonators	5.14-8.88	0.539	0.431	1.314
Pin-feed MSA	9.2-9.3	0.047	0.237	0.425

We observe that all non-resonant slot coupled antennas have similar performance, but hour-glass is better than the others. Resonant slot with two stacked patches achieves almost 54% BW.

IV. KU BAND ANTENNA

To corroborate simulation results, we built an hourglass shaped non-resonant slot coupled antenna shown in Fig. 7. Radiating and parasitic patches were formed on flexible PCB's with 0.075 mm thickness and placed over the slots using Rohacell HF 31 foam (ε_r=1.046, tanδ=0.0017). Prototype antenna element is shown in Fig. 8, where corners of patch elements cut for less antenna-to-antenna coupling in an array application. Target band is Ku-band downlink frequencies. Measurements were carried out in an anechoic chamber using R&S ZVA40 Network Analyzer, and measurement results are displayed in Fig. 9.

Simulations show that the antenna has maximum broadside gain of 9.67 dBi at 11.24 GHz. Measured antenna has 30% BW (10.2 to 13.6 GHz) and maximum broadside gain of 9.5 dBi. Broadside gain is greater than 9.0 dBi in 10.8-12.75 GHz frequency band. In band gain ripple is less than 0.5 dB, which is also desirable in phased array antenna applications. Vertical polarization principal plane (φ=0°) radiation pattern at 11.9 GHz, center frequency of Ku band downlink, is shown in Fig. 10. The HPBW is 80°. Imperfections in the measurement setup gave rise to small ripple at the broadside. Due to its wide beamwidth, the antenna can be utilized in electronically steered phased array antennas.

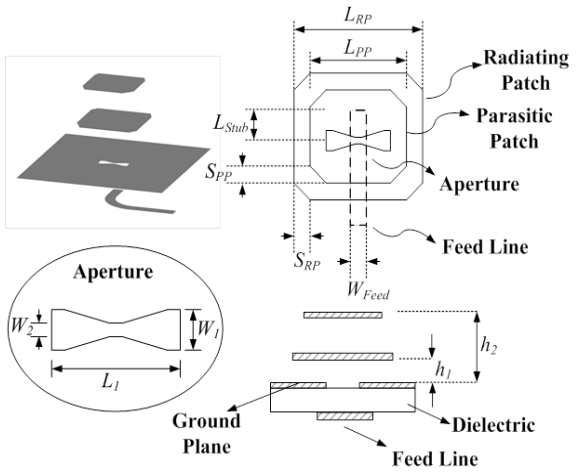

Fig. 7. Aperture coupled stacked microstrip patch antenna (L1=4.7 mm, W1=1.5 mm, W2=0.5 mm, LRP=10.8 mm, LPP=9.3 mm, SRP=1.7 mm, WFeed=1.1 mm).

Fig. 8. Antenna prototype: top (patch) side and bottom (feed line) side.

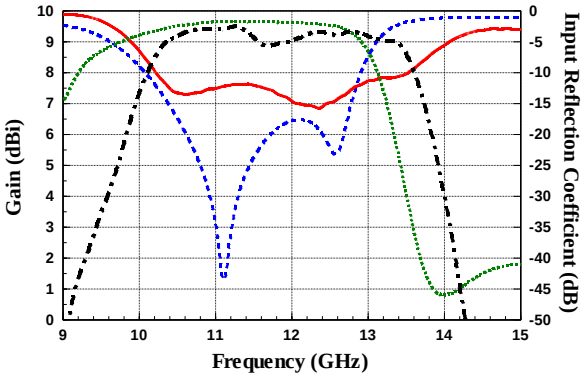

Fig. 9. Simulated and measured gain and input reflection coefficient of aperture coupled antenna (measured input reflection coefficient, measured gain, simulated gain, simulated input reflection coefficient).

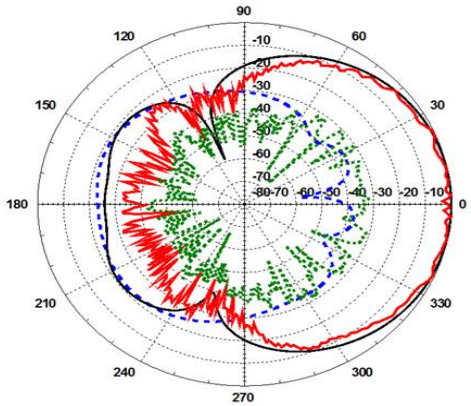

Fig. 10. Simulated and measured, normalized gain patterns at 11.5 GHz (measured co-pol pattern, simulated co-pol pattern, measured X-pol pattern, simulated X-pol pattern).

V. BENCHMARKING

In a typical system design minimum in-band gain is more critical than average gain to satisfy minimum target SNR. Hence, we modified FOM_1 in terms of minimum gain and electrical height of the antenna as:

$$FOM_2 = G_{min} BW \frac{1}{k_0 h}, \quad (18)$$

where G_{min} represents the minimum gain throughout the band and k_0h represents the electrical height at f_c. Electrical height of the antenna is a major factor in GBWP as discussed in Section II.

Finally, we define a third FOM to include HPBW as:

$$FOM_3 = G_{min} \left(\frac{HPBW}{\pi}\right) BW \frac{1}{k_0 h}, \quad (19)$$

where $HPBW$ is normalized to π. We did not include any front-to-back ratio parameter, as we are interested in receive-only system.

Although, prior work on aperture coupled antennas are abundant in the literature, we have selected those with either high gain or large BW [16-21]. In [16], two designs with and without superstrate layer were proposed and both were taken into consideration. In terms of FOM_1, [18] has the best performance, but since it employs frequency selective surfaces, its transverse dimensions are much larger than the others and it should be compared to an array antenna with the same size. Present work is better than all other designs in terms of FOM_2 and FOM_3 as shown in Table 2. We believe FOM_2 and FOM_3 are critical in array applications, as the height of the antenna can be further increased with suspended or inverted substrate-etched structures to enhance gain at the expense of increased antenna profile.

Table 2: Comparison of antennas

Antenna	Gain (dBi)	*BW*	*HPBW*/π	k_0h	FOM_1	FOM_2	FOM_3
This work	8-9.5	0.296	**0.438**	0.868	2.389	**2.118**	**0.929**
[6]	5-7	**0.525**	0.431	1.452	2.424	1.142	0.493
[7]	7-8.9	0.391	0.444	1.925	2.388	0.642	0.285
[8]	8.2-9.1	0.155	0.437	0.607	1.211	1.806	0.790
[16]	9-9.3	0.110	0.433	0.617	0.905	1.413	0.612
[16]	12-13.9	0.110	N/A	3.539	2.221	0.492	N/A
[17]	9.2-9.7	0.190	0.435	1.007	1.601	1.313	0.571
[18]	8-13.5	0.235	0.138	4.451	**3.485**	0.333	0.046
[19]	8.5-9.17	0.355	0.435	1.171	2.777	1.836	0.799
[20]	6.2-6.7	0.040	0.351	0.544	0.187	0.344	0.120

VI. CONCLUSIONS

We studied high gain, wideband aperture coupled antennas based on their GBWP's. Starting from pin-feed microstrip antenna, we showed that there exists an electrical height and aspect ratio where GBWP is optimal. We also showed that non-resonant slot shape (rectangular, hour-glass or any similar form) was not critical in terms of bandwidth, if the design was optimized properly. Similar but slightly worse performance was obtained with resonant slot coupled patch antenna. Resonant slot coupled with two stacked patches (3-resonator antenna) achieved 54% BW, but had inferior gain. Thus, resonant slot produces the best bandwidth, but less gain compared to non-resonant slot. In terms of GBWP, hour-glass shaped slot coupled antenna had the best result.

Hour-glass shape non-resonant slot coupled with two stacked patches was validated with measurements. Measured antenna has gain greater than 9.0 dBi throughout the downlink Ku-band. It exhibits less than 0.5 dB in band gain fluctuation, which helps the calibration of the array antenna that would be formed using it.

Several FOM's have been defined and the performance of the antenna is compared with those of previously published works. It is shown that proposed design outperforms earlier designs. We believe that the proposed antenna element can be used in demanding array applications where element gain, bandwidth, in band gain variation, and scan angle are among critical design specifications.

ACKNOWLEDGMENT

This work is partly funded by Trade, Commerce and Science Ministry of Turkey under Grant No. 439.STZ.2009-2 and NETA A.S, satellite equipment manufacturer based in Istanbul, Turkey. The authors would also like to thank FEKO EMSS GmbH for providing extended software license.

REFERENCES

[1] J. S. McLean, "A re-examination of the fundamental limits on the radiation q of electrically small antennas," *IEEE Trans. Antennas Propagat.*, vol. 44, pp. 672-676, May 1996.

[2] D. M. Pozar, "Microstrip antenna aperture-coupled to a microstripline," *Electronics Letters*, vol. 21, iss. 2, pp. 49-50, January 17 1985.

[3] G. Kumar and K. P. Ray, "Broadband microstrip patch antennas," *Artech House*, ch. 4, pp. 151-169, 2003.

[4] J. R. James and P. S. Hall, "Handbook of microstrip antennas," *IET*, 1989

[5] D. M. Pozar and S. D. Targonski, "Improved coupling for aperture-coupled microstrip antennas," *Electron. Lett.*, vol. 27, no. 13, pp. 1129-1131, 1991.

[6] S. D. Targonski, R. B. Waterhouse, and D. M. Pozar, "Wide-band aperture-coupled stacked patch antenna using thick substrate," *Electron. Lett.*, vol. 32, no. 21, pp. 1941-1942, 1996.

[7] A. A. Serra, P. Nepa, G. Manara, G. Tribellini, and S. Cioci, "A wide-band dual-polarized stacked patch antenna," *IEEE Antennas Wireless Propagat. Lett.*, vol. 6, pp. 141-143, 2007.

[8] F. Rostan, G. Gottwald, and E. Heidrich, "Wideband aperture-coupled microstrip patch array for satellite TV reception," *Proc. 8th International Conference on Antennas and Propagation*, vol. 1, pp. 190-193, 1993.

[9] M. M. Bilgic and K. Yegin, "Wideband high-gain aperture coupled antenna for ku band phased array antenna systems," *Microwave and Optical Technology Letter*, vol. 55, no. 6, June 2013.

[10] D. R. Jackson and N. G. Alexopoulos, "Simple approximate formulas for input resistance, bandwidth, and efficiency of a resonant rectangular

patch," *IEEE Trans. Antennas Propagat.*, vol. 39, no. 3, pp. 407-410, March 1991.

[11] A. E. Gera, "The radiation resistance of a microstrip element," *IEEE Trans. Antennas Propagat.*, vol. 38, iss. 4, pp. 568-570, April 1990.

[12] B. Das and K. Joshi, "Impedance of a radiating slot in the ground plane of a microstripline," *IEEE Trans. Antennas Propagat.*, vol. 30, no. 5, no. 13, pp. 922-926, 1982.

[13] M. Edimo, K. Mahdjoubi, A. Sharaiha, and T. Terret, "Simple circuit model for coax-fed stacked microstrip patch antenna," *IEE Proceedings Microwaves, Antennas and Propagation*, vol. 145, no. 3, pp. 268-272, 1998.

[14] M. Himdi, J. P. Daniel, and C. Terret, "Transmission line analysis of aperture-coupled microstrip antenna," *Electronics Letters*, vol. 25, no. 18, pp. 1229-1230, August 1989.

[15] H. Pues and A. Van de Capelle, "Accurate transmission-line model for the rectangular microstrip antenna," *IEE Proceedings Microwaves, Antennas and Propagation*, vol. 131, iss. 6, pp. 334-340, December 1984.

[16] W. Choi, Y. H. Cho, C. Pyo, and J. Choi, "A high-gain microstrip patch array antenna using a superstrate layer," *ETRI Journal*, vol. 25, no. 5, pp. 407-411, October 2003.

[17] W. Choi, J. M. Kim, J. H. Bae, and C. Pyo, "High gain and broadband microstrip array antenna using combined structure of corporate and series feeding," *Proc. IEEE Antennas Propagat. Soc. Int. Sym*., vol. 3, pp. 2484-2487, June 2004.

[18] A. Pirhadi, H. Bahrami, and J. Nasri, "Wideband high directive aperture coupled microstrip antenna design by using a FSS superstrate layer," *IEEE Trans. Antennas Propagat.*, vol. 60, no. 4, pp. 2101-2106, April 2012.

[19] J. Lee, C. Ahn, and K. Chang, "Broadband circularly polarized aperture-coupled microstrip antenna with dual-offset feedlines," *Proc. IEEE Int. Sym. Antennas Propagat.*, pp. 1127-1130, July 2011.

[20] P. Mousavi, et al., "A low-cost ultra-low profile phased array system for mobile satellite reception using zero-knowledge beamforming algorithm," *IEEE Trans. Antennas Propagat.*, vol. 56, no. 12, pp. 3667-3679, December 2008.

[21] M. H. Ullah, M. T. Islam, and F. S. Mandeep, "Printed prototype of a wideband s-shape microstrip patch antenna for ku/k band applications," *Appl. Comp. Electro. Society (ACES) Journal*, vol. 28, no. 4, pp. 307-313, April 2013.

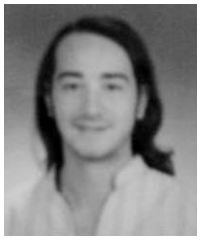

Mustafa Murat Bilgiç received his B.S., M.S. and Ph.D. degrees in Electrical and Electronics Eng. at Yeditepe University, Istanbul, Turkey in 2002, 2008, and 2014, respectively. He is currently working with Unitest Inc., Istanbul, Turkey. His main research interests are phased array antennas and wideband antennas.

Korkut Yeğin received his B.S. degree in Electrical and Electronics Eng. at Middle East Technical University, Ankara, Turkey in 1992, his M.S. and Ph.D. degrees in Electrical and Computer Engineering, Clemson University, SC in 1996 and 1999, respectively. He worked as a Post-doctoral Research Fellow at UIUC from 2000 to 2002 and as Advanced Development Engineer in Delphi Delco Electronics, MI from 2002 to 2007. He was with Yeditepe University Electrical and Electronics Eng. Dept., Istanbul, Turkey from 2007 to 2014. He is now with Electrical and Electronics Eng., Ege University, Izmir, Turkey. His main research interests are UWB radar, phased array antennas, and RF front-end circuits.